KSOE

Journal of Ocean Engineering and Technology 39(1), 32−39, February, 2025 eISSN 2287-6715
https://doi.org/10.26748/KSOE.2024.076

Original Research Article

Wave Transmission Analysis of Timoshenko Beam Junction with Mindlin Plates Connected in the Same Plane

Young-Ho Park[1]

[1]*Professor, Department of Smart Ocean Mobility Engineering, Changwon National University, Changwon, Korea*

KEYWORDS: Mindlin plate, Timoshenko beam, Energy flow analysis (EFA), Wave transmission analysis, Stiffened plate

ABSTRACT: *Energy flow analysis (EFA) models that account for significant shear deformation and the rotatory inertia effects in out-of-plane motion are essential for performing reliable EFA of practical composite structures, such as large ships or offshore platforms. The power coefficients for transmitted and reflected waves caused by incident waves at arbitrary angles in the incident Mindlin plate were derived by analyzing the displacement fields of semi-infinite Mindlin plates and an infinite Timoshenko beam. This enables the determination of the power transmission and reflection coefficients for diffuse fields, which are crucial for calculating the frequency-averaged vibrational power transfer relationship among coupled finite structures. The power transfer relationship, derived from the undamped wave solutions of the Mindlin plate and the Timoshenko beam, showed through numerical examples that the stiffening Timoshenko beam effectively insulates the Mindlin plate from out-of-plane vibrational power. Numerical analysis showed that the stiffening beam effectively blocks the vibrational power transmission of out-of-plane waves in the incident Mindlin plate. In addition, the power transmission and reflection tendencies of these waves vary with the cross-sectional size of the stiffening Timoshenko beam. This approach aims to enhance the reliability of vibrational analysis for stiffened plate structures.*

1. Introduction

Recent interest in the environment has surged because of global warming. The focus on applying carbon-free powertrains and reducing structural weight in vehicles, such as ships, automobiles, and aircraft, which are major sources of carbon emissions, has increased to enhance the sustainability of humanity. Generally, these changes in vehicles increase the significance of noise and vibration in the high-frequency range. In addition, ships and offshore platforms have relatively thicker structural members compared to other vehicles. Hence, the shear distortion effect and rotatory inertia effect in out-of-plane vibration become more significant.

At high frequencies, statistical approaches like the energy flow analysis (EFA) and the statistical energy analysis (SEA) are highly effective. They offer advantages in terms of analytical cost and the usability of prediction results compared to classical deterministic approaches such as finite element analysis (FEA) and boundary element analysis (BEA).

Although SEA uses the power balance equation in the form of a linear system of equations, EFA utilizes an energy-governing equation in the form of a partial differential equation. This allows EFA to be applied effectively to numerical techniques such as the finite element method (FEM) or the boundary element method (BEM), making it easier to model complex systems compared to SEA. EFA is a superior high-frequency analysis technique because it enables local vibration isolation and acoustical absorption treatment, improving noise and vibration control.

Research on EFA has focused primarily on two areas: developing energy flow models by deriving energy-governing equations for various structural and acoustic fundamental elements (bar, membrane, beam, plate, and acoustic cavity) (Belov et al., 1977; Bouthier and Bernhard, 1992, 1995; Cho, 1993; Kim et al., 1994; Nefske and Sung, 1989; Park et al., 2001; Park and Hong, 2006a, 2008; Wohlever and Bernhard, 1988), and deriving power transfer relationships at the junctions between these elements for EFA and SEA of coupled structures (Cho, 1993; Langley and Heron, 1990; Lyon and DeJong, 1994; Park, 2013, 2014; Seo et al., 2003). Significant progress has been made in both areas.

Numerical techniques are an application field of EFA. Representative examples include the energy flow finite element

Received 19 September 2024, revised 11 December 2024, accepted 12 December 2024
Corresponding author Young-Ho Park: +82-55-213-3684, parkyh@changwon.ac.kr

analysis (EFFEA) and the energy flow boundary element analysis (EFBEA). Various studies have applied numerical analysis techniques, such as FEM or BEM, to the results of the major research areas mentioned above, enabling the EFA of practical complex systems (Bernhard and Wang, 2008; Cho, 1993; Park, 2019; Teng et al., 2023). Recently, studies on Timoshenko beams and Mindlin plates using EFA have attracted interest. These studies consider the effects of rotatory inertia and shear deformation, which become significant at high frequencies and with increasing cross-sectional size. Park and Hong were pioneers in this field, separating three distinct waves from the equation of out-of-plane motion. They named these waves based on their characteristics: the out-of-plane shear wave (OPSW), the bending dominant flexural wave (BDFW), and the shear dominant flexural wave (SDFW). In addition, they derived the energy-governing equation for each wave (Park and Hong, 2006a, 2008).

Park conducted a power transfer analysis of a general point junction coupled with semi-infinite Timoshenko beams and performed EFA on composite structures composed of finite Timoshenko beams (Park and Hong, 2006b). Furthermore, to enhance the reliability of EFA for plate composite structures in the high-frequency range, wave transmission analysis was carried out for various line junctions coupled with semi-infinite Mindlin plates (Park, 2013, 2014).

Large-area thick plate structures, such as those used in ships and offshore platforms, often incorporate beams to enhance their out-of-plane stiffness. Consequently, several studies have been conducted to investigate the vibration characteristics of these stiffened plates (Aksu and Ali, 1976; Alaimo et al., 2019; Koko and Olson, 1992; Langley and Heron, 1990; Liu et al., 2019; Nokhbatolfoghahai et al., 2020; Seo et al., 2003; Yin et al., 2018). Among these studies, Langley and Heron (1990) conducted wave transmission analysis on a general line junction connected with Kirchhoff plates in a Timoshenko beam, and Seo et al. conducted wave transmission analysis of a general line junction connected with Kirchhoff plates in a Euler beam and performed EFA on this simple structures. Liu et al. calculated the vibration power of Mindlin plates stiffened with Timoshenko beams using an exact solution and compared it with the FEA results. For reliable EFA of large-area stiffened thick plates at high frequencies, it is essential to determine the power transmission and reflection coefficients for various types of waves presented in the Mindlin plate. This crucial aspect has not been adequately addressed in previous studies.

This study conducted wave transmission analysis of a line junction connected with co-planar Mindlin plates in a Timoshenko beam. The analysis used the undamped exact solutions of each structural element.

2. Mindlin Plate Theory and Timoshenko Beam Theory

2.1 Equations of Out-of-plane Motions for Undamped Mindlin Plate

At high frequencies, the shear distortion effect and the rotatory inertia effect, which are ignored in the Kirchhoff plate theory, become very important in the vibration response. The equations of out-of-plane motions of the Mindlin plate, which include these effects, are expressed as follows (Park and Hong, 2008):

$$D_p\left[\frac{\partial^2\alpha_{p,x}}{\partial x^2}+\frac{(1-\nu_p)}{2}\frac{\partial^2\alpha_{p,x}}{\partial y^2}+\frac{(1+\nu_p)}{2}\frac{\partial^2\alpha_{p,y}}{\partial x\partial y}\right] - x_pG_ph_p\left(\alpha_{p,x}+\frac{\partial w_p}{\partial x}\right)=\rho_pI_p\frac{\partial^2\alpha_{p,x}}{\partial t^2} \tag{1}$$

$$D_p\left[\frac{\partial^2\alpha_{p,y}}{\partial y^2}+\frac{(1-\nu_p)}{2}\frac{\partial^2\alpha_{p,y}}{\partial x^2}+\frac{(1+\nu_p)}{2}\frac{\partial^2\alpha_{p,x}}{\partial x\partial y}\right] - x_pG_ph_p\left(\alpha_{p,y}+\frac{\partial w_p}{\partial y}\right)=\rho_pI_p\frac{\partial^2\alpha_{p,y}}{\partial t^2} \tag{2}$$

$$x_pG_ph_p\left(\frac{\partial\alpha_{p,x}}{\partial x}+\frac{\partial\alpha_{p,y}}{\partial y}+\frac{\partial^2w_p}{\partial x^2}+\frac{\partial^2w_p}{\partial y^2}\right)=\rho_ph_p\frac{\partial^2w_p}{\partial t^2} \tag{3}$$

where w_p is the transverse displacement; $\alpha_{p,x}$ and $\alpha_{p,y}$ are the rotational angles about each axis due to bending; h_p is the thickness of the plate; $I_p=h_p^3/12$ is the moment of inertia per unit length; D_p is the flexural rigidity; E_p is the elastic modulus; ν_p is Poisson's ratio; $x_p=20(1+\nu_p)/(24+25\nu_p+\nu_p^2)$ is the shear correction factor; ρ_p is the mass density; G_p represents the shear modulus.

The wavenumbers of the waves existing in the Mindlin plate can be obtained by applying the displacement potential functions ϕ and ψ to the equations of out-of-plane motion of the Mindlin plate, as follows (Park and Hong, 2008):

$$k_{p1}=\sqrt{(\rho_pI_p\omega^2)/G_pI_p} \tag{4}$$

$$k_{p2}=\sqrt{\frac{\rho_p\omega^2}{2}\left(\frac{1}{x_pG_p}+\frac{I_p}{D_p}\right)+\sqrt{\frac{\rho_p^2\omega^4}{4}\left(\frac{1}{x_pG_p}-\frac{I_p}{D_p}\right)+\frac{\rho_ph_p\omega^2}{D_p}}} \tag{5}$$

$$k_{p3}=\sqrt{\frac{\rho_p\omega^2}{2}\left(\frac{1}{x_pG_p}+\frac{I_p}{D_p}\right)-\sqrt{\frac{\rho_p^2\omega^4}{4}\left(\frac{1}{x_pG_p}-\frac{I_p}{D_p}\right)+\frac{\rho_ph_p\omega^2}{D_p}}} \tag{6}$$

where k_{p1}, k_{p2}, and k_{p3} are the OPSW, BDFW, and SDFW of the Mindlin plate, respectively.

2.2 Equations of Out-of-plane Motions for Undamped Timoshenko Beam

The equations of motions for the transverse bending of the Timoshenko beam, which reflect the shear distortion effect and rotatory inertia effect important at high frequencies, similar to the Mindlin plate, are as follows (Park and Hong, 2006a):

$$E_bI_bA_b\frac{\partial^2\alpha_b}{\partial y^2}-x_bG_bA_b\left(\frac{\partial w_b}{\partial y}+\alpha_b\right)=\rho_bI_b\frac{\partial^2\alpha_b}{\partial t} \tag{7}$$

$$-\varkappa_b G_b A_b\left(\frac{\partial^2 w_b}{\partial y^2}+\frac{\partial \alpha_b}{\partial y}\right)=\rho_b A_b \frac{\partial^2 w_b}{\partial t} \tag{8}$$

where w_b is the transverse displacement; α_b is the rotational angle due to bending; $A_b = h_b \times b_b$ is the cross-sectional area; h_b is the height; b_b is the breadth of the beam; $I_b = b_b h_b^3/12$ is the moment of inertia per unit length; E_b is the elastic modulus; $\varkappa_b = 20(1+\nu_b)/(24+25\nu_b+\nu_b^2)$ is the shear correction factor; ρ_b is the mass density; G_b is the shear modulus of the beam.

As with the Mindlin plate, the Timoshenko beam also exhibits BDFWs and SDFWs as propagating waves above the critical frequency ($\omega_{c,b} = \sqrt{\varkappa_b G_b A_b/\rho_b I_b}$). Below the critical frequency, only the bending dominant flexural wave exists as a propagating wave, similar to the Euler beam. The wavenumbers of each wave are as follows:

$$k_{b1} = \sqrt{\frac{\rho_b\omega^2}{2}\left(\frac{1}{\varkappa_b G_b}+\frac{I_b}{E_b}\right)+\sqrt{\frac{\rho_b^2\omega^4}{4}\left(\frac{1}{\varkappa_b G_b}-\frac{I_b}{E_b}\right)+\frac{\rho_b A_b\omega^2}{E_b I_b}}} \tag{9}$$

$$k_{b2} = \sqrt{\frac{\rho_b\omega^2}{2}\left(\frac{1}{\varkappa_b G_b}+\frac{I_b}{E_b}\right)-\sqrt{\frac{\rho_b^2\omega^4}{4}\left(\frac{1}{\varkappa_b G_b}-\frac{I_b}{E_b}\right)+\frac{\rho_b A_b\omega^2}{E_b I_b}}} \tag{10}$$

where k_{b1} and k_{b2} represent the BDFW and SDFW of the Timoshenko beam, respectively.

3. Wave Transmission Analysis of Semi-Infinite Co-planar Mindlin Plates Stiffened with a Timoshenko Beam

3.1 Wave Solutions of Mindlin Plate and Timoshenko Beam

Fig. 1 shows semi-infinite co-planar Mindlin plates stiffened with an infinite Timoshenko beam. The in-plane wave can be ignored if the stiffened plate is in the same plane. Accordingly, the wave field of the incident Mindlin plate can be expressed as follows (Park, 2013; Park and Hong, 2008):

$$\psi_{p,i}(x,y,t) = \left\{{}_i e^{(-jk_{p1x,i}x - jk_{p1y,i}y)} + B_i e^{(jk_{p1x,i}x - jk_{p1y,i}y)}\right\} e^{j\omega t} \tag{11}$$

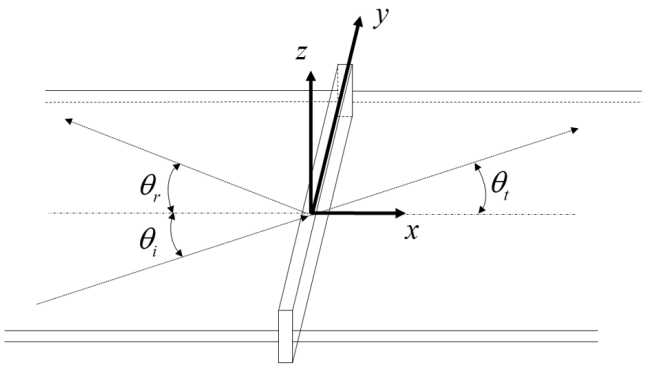

Fig. 1 Semi-infinite co-planar Mindlin plates stiffened with an infinite Timoshenko beam.

$$\begin{Bmatrix}\phi_{p,i}\\ w_{p,i}\end{Bmatrix}(x,y,t) = \left[\begin{Bmatrix}\rho_{p,i}h_{p,i}\omega^2 - \varkappa_{p,i}G_{p,i}h_{p,i}k_{p2,i}^2\\ \varkappa_{p,i}G_{p,i}h_{p,i}k_{p2,i}^2\end{Bmatrix}\left({}_i e^{(-jk_{p2x,i}x - jk_{p2y,i}y)} + D_i e^{(jk_{p2x,i}x - jk_{p2y,i}y)}\right)\right.$$
$$\left. + \begin{Bmatrix}\rho_{p,i}h_{p,i}\omega^2 - \varkappa_{p,i}G_{p,i}h_{p,i}k_{p3,i}^2\\ \varkappa_{p,i}G_{p,i}h_{p,i}k_{p3,i}^2\end{Bmatrix}\left({}_i e^{(-jk_{p3x,i}x - jk_{p3y,i}y)} + F_i e^{(jk_{p3x,i}x - jk_{p3y,i}y)}\right)\right] e^{j\omega t} \tag{12}$$

where the subscript 'i' indicates the incident plate; k_{px} and k_{py} are the x- and y-directional components of each wavenumber, respectively; $\psi_{p,i}$ is a displacement potential function that only has the characteristics of OPSW; $\phi_{p,i}$ and $w_{p,i}$ are the displacement potential function and the z-directional displacement, respectively, which have the characteristics of BDFW and SDFW. The overbar of the coefficient of each wave field indicates the incident wave.

In the incident plate, the incident waves and reflected waves exist as described in Eqs. (11)–(12), but only transmitted waves exist in the transmitted plate. Therefore, the wave field in the transmitted plate can be expressed as follows:

$$\psi_{p,t}(x,y,t) = G_t e^{(-jk_{p1x,t}x - jk_{p1y,t}y)} e^{j\omega t} \tag{13}$$

$$\begin{Bmatrix}\phi_{p,t}\\ w_{p,t}\end{Bmatrix}(x,y,t) = \left[\begin{Bmatrix}\rho_{p,t}h_{p,t}\omega^2 - \varkappa_{p,t}G_{p,t}h_{p,t}k_{p2,t}^2\\ \varkappa_{p,t}G_{p,t}h_{p,t}k_{p2,t}^2\end{Bmatrix}\left(H_t e^{(-jk_{p2x,t}x - jk_{p2y,t}y)}\right)\right.$$
$$\left. + \begin{Bmatrix}\rho_{p,t}h_{p,t}\omega^2 - \varkappa_{p,t}G_{p,t}h_{p,t}k_{p3,t}^2\\ \varkappa_{p,t}G_{p,t}h_{p,t}k_{p3,t}^2\end{Bmatrix}\left(I_t e^{(-jk_{p3x,t}x - jk_{p3y,t}y)}\right)\right] e^{j\omega t} \tag{14}$$

where the subscript 't' indicates the transmitted plate.

An out-of-plane wave incident at an arbitrary angle on the incident plate generates a wave field in the Timoshenko beam, including a torsional wave, as follows (Park and Hong, 2006a, 2006b):

$$w_b(y,t) = L_b e^{(-jk_{by}y)} e^{j\omega t} \tag{15}$$

$$\alpha_b(y,t) = M_b e^{(-jk_{by}y)} e^{j\omega t} \tag{16}$$

$$\theta_b(y,t) = N_b e^{(jk_{by}y)} e^{j\omega t} \tag{17}$$

where w_b, α_b, and θ_b are the z-direction displacement, rotation angle about the x-axis, and twist angle about the y-axis of the stiffening beam, respectively.

In Eqs. (15)–(17), the wavenumber k_b has the following relationship due to the y-directional wavenumber matching:

$$k_b = k_{p1y,i} = k_{p2y,i} = k_{p3y,i} = k_{p1y,t} = k_{p2y,t} = k_{p3y,t} \tag{18}$$

3.2 Wave Transmission Analysis of Co-planer Semi-infinite Mindlin Plates Reinforced with a Timoshenko Beam

Fig. 2 presents a cross-section of semi-infinite Mindlin plates stiffened with a Timoshenko beam placed on the same plane. The term 'plates placed on the same plane' suggests that the mid-surfaces of two plates with the same thickness are coincident. The stiffening beam was

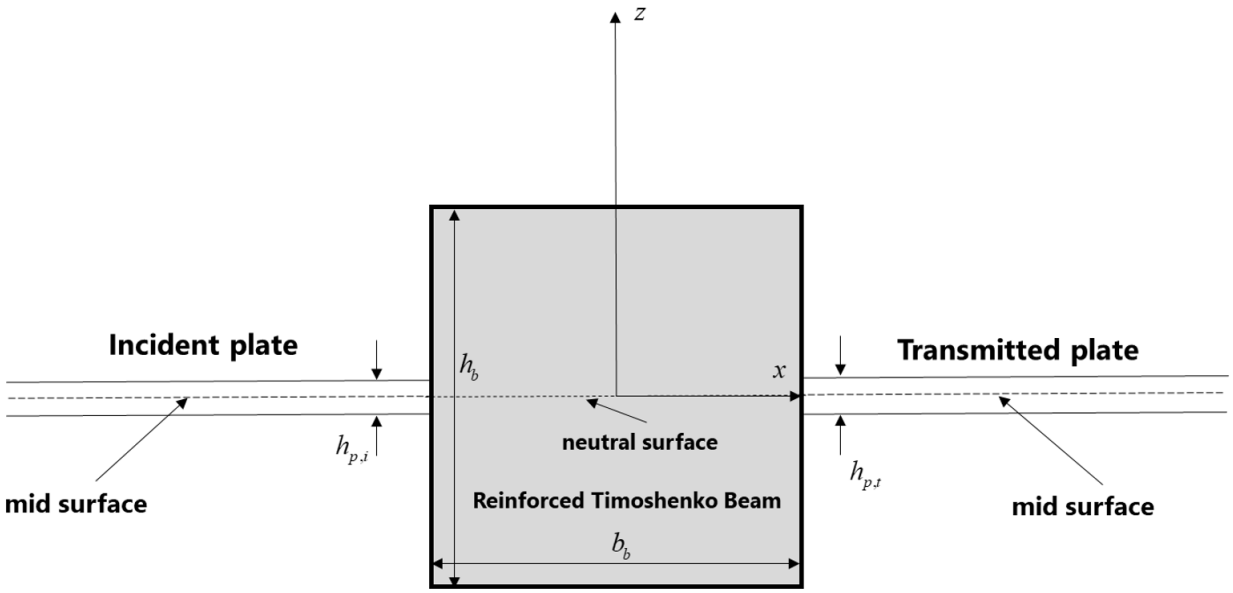

Fig. 2 Cross-section of the co-planar semi-infinite Mindlin plate structure stiffened with Timoshenko beam.

assumed to have a rectangular cross-section, with the neutral surface aligning with the mid-surfaces of the plates.

In a semi-infinite plate structure like Fig. 2, nine unknowns exist when one type of incident wave is present. The following six displacement continuity conditions and three force and moment equilibrium equations are required to determine these unknowns:

$$w_{p,i} = w_{p,t} = w_b \tag{19}$$

$$\alpha_{x,p,i} = \alpha_{x,p,t} = \theta_b \tag{20}$$

$$\alpha_{y,p,i} = \alpha_{y,p,t} = \alpha_b \tag{21}$$

$$\varkappa_b G_b A_b \left(\frac{\partial^2 w_b}{\partial y^2} + \frac{\partial \alpha_b}{\partial y} \right) - \rho_b A_b \omega^2 w_b = Q_{x,p,t} - Q_{x,p,i} \tag{22}$$

$$G_b J_b \frac{\partial^2 \theta_b}{\partial y^2} + \rho_b J_b \omega^2 \theta_b = M_{xx,p,t} - M_{xx,p,i} \tag{23}$$

$$E_b I_b A_b \frac{\partial^2 \alpha_{b,y}}{\partial y^2} - \varkappa_b G_b A_b \left(\frac{\partial w_b}{\partial y} + \alpha_{b,y} \right) + \rho_b I_b \omega^2 \alpha_{b,y} = M_{xy,p,t} - M_{xy,p,i} \tag{24}$$

where J_b is the torsional moment of inertia of the beam, the rotational angles $\alpha_{x,p} = \partial \phi_p / \partial x + \partial \psi_p / \partial y$ and $\alpha_{y,p} = \partial \phi_p / \partial y - \partial \psi_p / \partial x$ in the Mindlin plate are expressed using displacement potential functions. The internal shear force $Q_{x,p} = \varkappa_p G_p h_p (\partial w_p / \partial x + \alpha_{x,p})$, internal moments $M_{xx,p} = D_p (\partial \alpha_{x,p} / \partial x + \nu_p \, \partial \alpha_{y,p} / \partial y)$, and $M_{xy,p} = \{(1-\nu_p)/2\} D_p (\partial \alpha_{x,p} / \partial y + \partial \alpha_{y,p} / \partial x)$ are expressed using the displacement field valuables.

The unknown coefficients of all waves in the structure, when each known wave is incident on the incident plate, can be obtained using Eqs. (19)–(24).

3.3 Power Transfer Relationship of Co-planar Semi-infinite Mindlin Plates Stiffened with a Timoshenko Beam

As mentioned above, analyzing the EFA of complex structures requires deriving the power transfer relationship between each structural element. For the EFA of Mindlin plate structures stiffened with Timoshenko beams, the power transmission coefficients and power reflection coefficients in the diffuse field can be obtained using the wave transmission analysis results obtained previously, as follows:

$$P_{OPSW,i}^{inc} = \frac{1}{2} \left[\frac{D_{p,i}}{2} (1-\nu_{p,i}) \omega k_{p1x,i} k_{p1,i}^2 \right] \times |\overline{A}|^2 \tag{25}$$

$$P_{OPSW,i}^{refl} = \frac{1}{2} \left[\frac{D_{p,i}}{2} (1-\nu_{p,i}) \omega k_{p1x,i} k_{p1,i}^2 \right] \times |B|^2 \tag{26}$$

$$P_{BDFW,i}^{inc} = \frac{1}{2} \left[D_{p,i} \left(\rho_{p,i} h_{p,i} \omega^2 - \varkappa_{p,i} G_{p,i} h_{p,i} k_{p2,i}^2 \right)^2 \omega k_{p2x,i} k_{p2,i}^2 + \left(\rho_{p,i} h_{p,i} \omega^2 \right) \left(\omega k_{p2x,i} \right) \left(\varkappa_{p,i} G_{p,i} h_{p,i} k_{p2,i} \right)^2 \right] \times |\overline{C}|^2 \tag{27}$$

$$P_{BDFW,i}^{refl} = \frac{1}{2} \left[D_{p,i} \left(\rho_{p,i} h_{p,i} \omega^2 - \varkappa_{p,i} G_{p,i} h_{p,i} k_{p2,i}^2 \right)^2 \omega k_{p2x,i} k_{p2,i}^2 + \left(\rho_{p,i} h_{p,i} \omega^2 \right) \left(\omega k_{p2x,i} \right) \left(\varkappa_{p,i} G_{p,i} h_{p,i} k_{p2,i} \right)^2 \right] \times |D|^2 \tag{28}$$

$$P_{SDFW,i}^{inc} = \frac{1}{2} \left[D_{p,i} \left(\rho_{p,i} h_{p,i} \omega^2 - \varkappa_{p,i} G_{p,i} h_{p,i} k_{p3,i}^2 \right)^2 \omega k_{p3x,i} k_{p3,i}^2 + \left(\rho_{p,i} h_{p,i} \omega^2 \right) \left(\omega k_{p3x,i} \right) \left(\varkappa_{p,i} G_{p,i} h_{p,i} k_{p3,i} \right)^2 \right] \times |\overline{E}|^2 \tag{29}$$

$$P_{SDFW,i}^{refl} = \frac{1}{2} \left[D_{p,i} \left(\rho_{p,i} h_{p,i} \omega^2 - \varkappa_{p,i} G_{p,i} h_{p,i} k_{p3,i}^2 \right)^2 \omega k_{p3x,i} k_{p3,i}^2 + \left(\rho_{p,i} h_{p,i} \omega^2 \right) \left(\omega k_{p3x,i} \right) \left(\varkappa_{p,i} G_{p,i} h_{p,i} k_{p3,i} \right)^2 \right] \times |F|^2 \tag{30}$$

$$P_{OPSW,t}^{trans} = \frac{1}{2}\left[\frac{D_{p,t}}{2}(1-\nu_{p,t})\omega k_{p1x,t}k_{p1,t}^2\right]\times|G|^2 \quad (31)$$

$$P_{BDFW,t}^{trans} = \frac{1}{2}\left[D_{p,t}\left(\rho_{p,t}h_{p,t}\omega^2 - x_{p,t}G_{p,t}h_{p,t}k_{p2,t}^2\right)^2\omega k_{p2x,t}k_{p2,t}^2 + \left(\rho_{p,t}h_{p,t}\omega^2\right)\left(\omega k_{p2x,t}\right)\left(x_{p,t}G_{p,t}h_{p,t}k_{p2,t}\right)^2\right]\times|H|^2 \quad (32)$$

$$P_{SDFW,t}^{trans} = \frac{1}{2}\left[D_{p,t}\left(\rho_{p,t}h_{p,t}\omega^2 - x_{p,t}G_{p,t}h_{p,t}k_{p3,t}^2\right)^2\omega k_{p3x,t}k_{p3,t}^2 + \left(\rho_{p,t}h_{p,t}\omega^2\right)\left(\omega k_{p3x,t}\right)\left(x_{p,t}G_{p,t}h_{p,t}k_{p3,t}\right)^2\right]\times|I|^2 \quad (33)$$

The power transfer relationship of frequency-averaged vibrational power in the high-frequency band of a finite structure is represented by the power transfer relationship in the diffuse field of a semi-infinite structure (Cho, 1993). Using the vibrational power obtained from Eqs. (25)–(33), the following equations can be applied to determine the power transmission and reflection coefficients in the diffuse field:

$$\tau_{mn}(\theta) = \frac{P_{n,t}^{trans}(\theta)}{P_{m,i}^{inc}(\theta)}, \quad \gamma_{mn}(\theta) = \frac{P_{n,i}^{refl}(\theta)}{P_{m,i}^{inc}(\theta)},$$

$$\tau_{mn}^{D} = \int_0^{\pi/2}\tau_{mn}(\theta)\sin 2\theta d\theta, \quad \gamma_{mn}^{D} = \int_0^{\pi/2}\gamma_{mn}(\theta)\sin 2\theta d\theta \quad (34\text{-}37)$$

where $\tau_{mn}(\theta)$ and $\gamma_{mn}(\theta)$ represent the power transmission and reflection coefficients, respectively, when an "m"-type wave is incident on a line junction at an angle of θ and is transmitted or reflected as an "n"-type wave. The superscript "D" in the power transmission and reflection coefficients indicates the power transfer coefficient in the diffuse field.

4. Numerical Examples

4.1 Co-planar Semi-infinite Mindlin Plate Structure Stiffened with a Timoshenko Beam

In the first numerical example, the materials of the Mindlin plates and the Timoshenko beam were steel ($E = 2.1 \times 10^{10}$ Pa, $\rho = 7850$

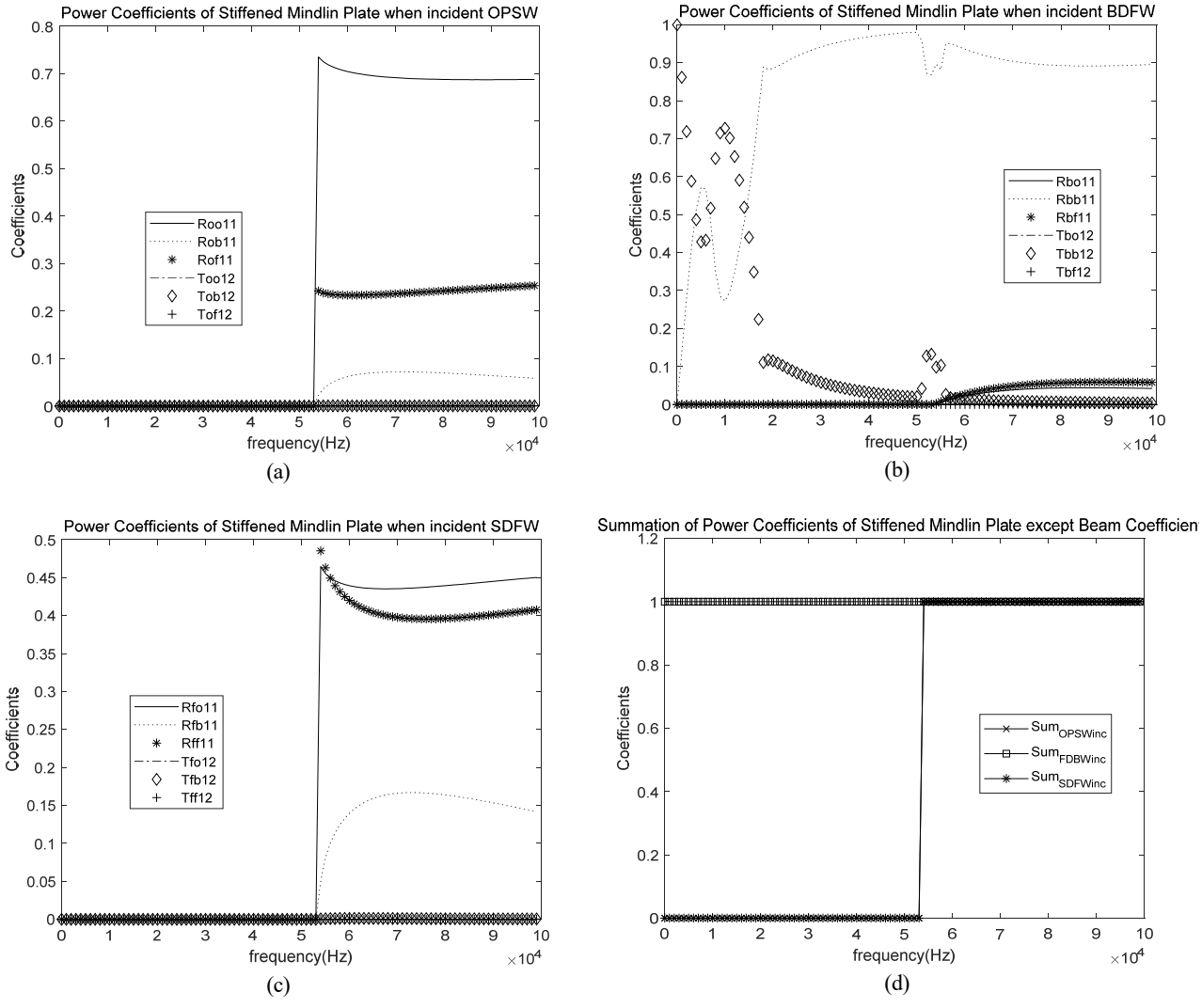

Fig. 3 Power coefficients of the first numerical example for the incident OPSW, BDFW, and SDFW: (a) for incident OPSW; (b) for incident BDFW; (c) for incident SDFW; (d) Summation of the power coefficients for each incident wave

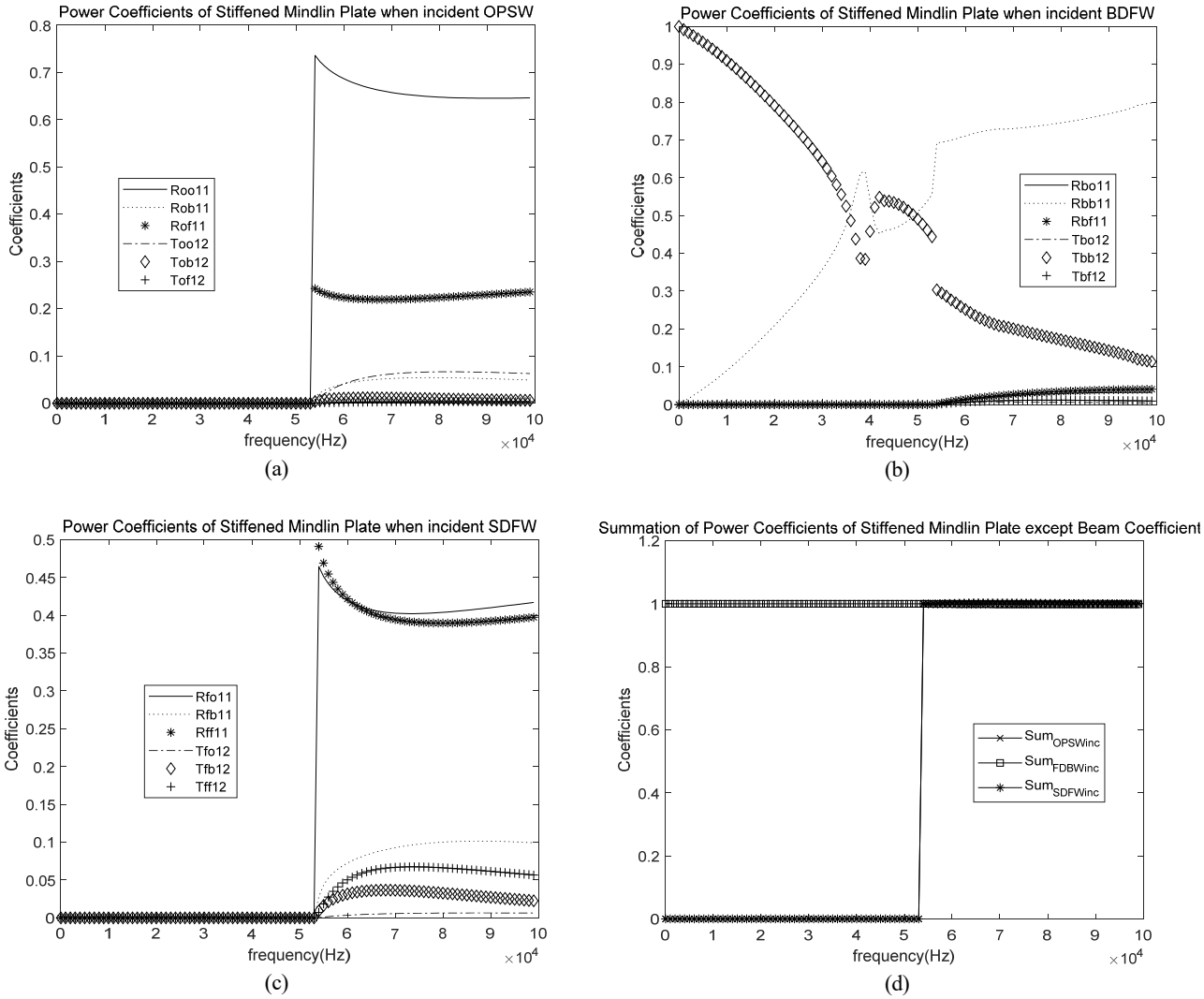

Fig. 4 Power coefficients of the second numerical example for incident OPSW, BDFW, and SDFW: (a) For incident OPSW; (b) For incident BDFW; (c) For incident SDFW; (d) Summation of power coefficients when each incident wave.

kg/m^3, $\nu = 0.3$). The thickness of the incident plate and the transmitted plate was assumed to be $h_{p,i} = h_{p,t} = 0.03$ m, and the height and breadth of the stiffening beam were assumed to be $h_b = 0.1$ m and $b_b = 0.03$ m, respectively. The critical frequency of the Mindlin plate in this example was 5.3479×10^4 Hz.

Fig. 3 presents the power transmission and reflection coefficients for each wave when it encounters a stiffening Timoshenko beam. As the critical frequency of the incident plate was approximately 53kHz, all power transmission and reflection coefficients were 0 when the OPSW and SDFW were incident. When there was no stiffening Timoshenko beam, the plates of the same material and thickness were connected on the same plane. Hence, no reflected waves occurred, and the power transmission coefficient became 1. Most of the incident power is reflected due to the effect of the stiffening Timoshenko beam (Figs. 3(a)–(c)). In the case of BDFW in Fig. 3(b), the transmitted power was more dominant than the reflected power despite the effect of the stiffening Timoshenko beam in the relatively low-frequency band. The first numerical example showed that the stiffening beam was quite effective in insulating the vibrational power of out-of-plane waves in the high-frequency band. The total sum of the power transfer coefficients was one across the entire frequency band because the stiffening Timoshenko beam is a joint where vibrational power is preserved (Fig. 3(d)).

In the second numerical example, wave transmission analysis was conducted on a model with a reduced cross-sectional size ($b_b \times h_b = 0.01$ m $\times$ 0.05 m) of the stiffening Timoshenko beam compared to the first numerical example. The vibrational power insulation effect was reduced due to the smaller cross-section of the stiffening Timoshenko beam (Fig. 4). The transmitted power increased compared to the first numerical example when all types of waves were incident (Fig. 4).

5. Conclusions

A prediction technique that incorporates the effects of shear deformation and rotatory inertia in out-of-plane vibrations is essential for enhancing the reliability of vibrational analysis for large-area

thick-plate structures at high frequencies. Therefore, the energy flow models for the Mindlin plate and Timoshenko beam are highly suitable analysis techniques for predicting vibrational and acoustical energetics in large ships and offshore platforms at high frequencies. In this study, wave transmission analysis was conducted to establish the power transfer relationship for the line junction connecting the Mindlin plates to the Timoshenko beam. This analysis is crucial for the EFA of stiffened plate structures, which are predominantly used in large ships and offshore platforms. The power transmission and reflection coefficients for the diffused field of each wave incident on the Mindlin plate were derived using the wave solution for the undamped semi-infinite Mindlin plate and the Timoshenko beam. The validity of the derived power transfer relationship was verified using several numerical examples. Applying stiffening beams is an effective method for insulating the propagation of out-of-plane vibrations in plate structures. In the future, energy flow analysis for simple stiffened plate structures should be conducted using the wave transfer relationship established in this paper. In addition, it is necessary to develop an energy flow finite element model to apply EFA to actual composite structures composed of stiffened plates.

Conflict of Interest

No potential conflict of interest relevant to this article was reported.

References

Aksu, G., & Ali, R. (1976). Free vibration analysis of stiffened plates using finite difference method. *Journal of Sound and Vibration*, *48*(1), 15−25. https://doi.org/10.1016/0022-460X(76)90367-9

Alaimo, A., Orlando, C., & Valvano, S. (2019). An alternative approach for modal analysis of stiffened thin-walled structures with advanced plate elements. *European Journal of Mechanics - A/Solids*, *77*, 103820. https://doi.org/10.1016/j.euromechsol.2019.103820

Belov, V. D., Rybak, S. A., & Tartakovskii, B. D. (1977). Propagation of vibrational energy in absorbing structures. *Physics Acoustics-USSR*, *23*(2), 115−119.

Bernhard, R., & Wang, S. (2008). Energy finite element method. In S. Marburg & B. Nolte (Eds.), *Computational Acoustics of Noise Propagation in Fluids—Finite and Boundary Element Methods* (pp. 287−306). Springer. https://doi.org/10.1007/978-3-540-77448-8_11

Bouthier, O. M., & Bernhard, R. J. (1992). Models of space-averaged energetics of plates. *AIAA Journal*, *30*(3), 616−623. https://doi.org/10.2514/3.10964

Bouthier, O. M., & Bernhard, R. J. (1995). Simple models of the energetics of transversely vibrating plates. *Journal of Sound and Vibration*, *182*(1), 149−164. https://doi.org/10.1006/jsvi.1995.0187

Cho, P. E.-H. (1993). *Energy flow analysis of coupled structures*. Purdue University ProQuest Dissertations & Theses.

Kim, H. S., Kang, H. J., & Kim, J. S. (1994). A vibration analysis of plates at high frequencies by the power flow method. *Journal of Sound and Vibration*, *174*(4), 493−504. https://doi.org/10.1006/jsvi.1994.1290

Koko, T. S., & Olson, M. D. (1992). Vibration analysis of stiffened plates by super elements. *Journal of Sound and Vibration*, *158*(1), 149−167. https://doi.org/10.1016/0022-460X(92)90670-S

Langley, R. S., & Heron, K. H. (1990). Elastic wave transmission through plate/beam junctions. *Journal of Sound and Vibration*, *143*(2), 241−253. https://doi.org/10.1016/0022-460X(90)90953-W

Liu, C., Zhang, J., & Li, F. (2019). Power transmission and suppression characteristics of stiffened Mindlin plate under different boundary constraints. *Archive of Applied Mechanics*, *89*(9), 1705−1721. https://doi.org/10.1007/s00419-019-01538-9

Lyon, R. H., & DeJong, R. G. (1994). *Theory and application of statistical energy analysis* (2nd ed.). Elsevier Science. https://doi.org/10.1016/C2009-0-26747-X

Nefske, D. J., & Sung, S. H. (1989). Power flow finite element analysis of dynamic systems: Basic theory and application to beams. *Journal of Vibration, Acoustics, Stress, and Reliability in Design*, *111*(1), 94−100. https://doi.org/10.1115/1.3269830

Nokhbatolfoghahai, A., Navazi, H., & Haddadpour, H. (2020). High-frequency random vibrations of a stiffened plate with a cutout using energy finite element and experimental methods. *Proceedings of the Institution of Mechanical Engineers, Part C: Journal of Mechanical Engineering Science*, *234*(16), 3297−3317. https://doi.org/10.1177/0954406220914328

Park, D.-H., Hong, S.-Y., Kil, H.-G., & Jeon, J.-J. (2001). Power flow models and analysis of in-plane waves in finite coupled thin plates. *Journal of Sound and Vibration*, *244*(4), 651−668. https://doi.org/10.1006/jsvi.2000.3517

Park, Y.-H. (2013). Wave transmission analysis of co-planar coupled semi-infinite Mindlin plate. *Transactions of the Korean Society for Noise and Vibration Engineering*, *23*(6), 574−580. https://doi.org/10.5050/KSNVE.2013.23.6.574

Park, Y.-H. (2014). Wave transmission analysis of semi-infinite Mindlin plates coupled at an arbitrary angle. *Transactions of the Korean Society for Noise and Vibration Engineering*, *24*(12), 999−1006. https://doi.org/10.5050/KSNVE.2014.24.12.999

Park, Y.-H. (2019). Energy flow finite element analysis of general Mindlin plate structures coupled at arbitrary angles. *International Journal of Naval Architecture and Ocean Engineering*, *11*(1), 435−447. https://doi.org/10.1016/j.ijnaoe.2018.08.001

Park, Y.-H., & Hong, S.-Y. (2006a). Vibrational energy flow analysis of corrected flexural waves in Timoshenko beam − Part I: Theory of an energetic model. *Shock and Vibration*, *13*(3), 308715. https://doi.org/10.1155/2006/308715

Park, Y.-H., & Hong, S.-Y. (2006b). Vibrational energy flow analysis of corrected flexural waves in Timoshenko beam − Part II: Application to coupled Timoshenko beams. *Shock and Vibration*,

13(3), 562762. https://doi.org/10.1155/2006/562762

Park, Y.-H., & Hong, S.-Y. (2008). Vibrational power flow models for transversely vibrating finite Mindlin plate. *Journal of Sound and Vibration*, *317*(3), 800−840. https://doi.org/10.1016/j.jsv.2008.03.049

Seo, S.-H., Hong, S.-Y., & Kil, H.-G. (2003). Power flow analysis of reinforced beam-plate coupled structures. *Journal of Sound and Vibration*, *259*(5), 1109−1129. https://doi.org/10.1006/jsvi.2002.5118

Teng, X., Han, Y., Jiang, X., Chen, X., & Zhou, M. (2023). Energy flow analysis model of high-frequency vibration response for plates with free layer damping treatment. *Mathematics*, *11*(6), 1379. https://doi.org/10.3390/math11061379

Wohlever, J. C., & Bernhard, R. J. (1988). *Vibrational power flow analysis of rods and beams* (No. NAS 1.26:183166). https://ntrs.nasa.gov/citations/19880020767

Yin, X., Wu, W., Zhong, K., & Li, H. (2018). Dynamic stiffness formulation for the vibrations of stiffened plate structures with consideration of in-plane deformation. *Journal of Vibration and Control*, *24*(20), 4825−4838. https://doi.org/10.1177/1077546317735969

Author ORCID

Author name	ORCID
Park, Young-Ho	0000-0001-8614-4897